Lasers in Surgery and Medicine 24:14–23 (1999)

Histopathological Features of Liver Damage Induced by Laser Ablation in Rabbits

Yutaka Fujitomi, MD,[1] Kenji Kashima, MD, PhD,[2] Shinnya Ueda, MD,[3] Yasunari Yamada, MD,[3] Hiromu Mori, MD, PhD,[3]* and Yuzo Uchida, MD, PhD[1]

[1]Second Department of Surgery, Oita Medical University, Oita 879-5593, Japan
[2]First Department of Pathology, Oita Medical University, Oita 879-5593, Japan
[3]Department of Radiology, Oita Medical University, Oita 879-5593, Japan

Background and Objective: **Possible mechanisms that promote or interfere with the effects of laser ablation of the liver have not been clarified. The aim of this study was to define the chronological alterations in the normal rabbit liver at early stages after laser ablation.**
Study Design/Materials and Methods: **Rabbit livers were ablated with a laser via an optical fiber and then analyzed histopathologically by immunostaining for heat shock protein 70 (HSP70) and by the terminal deoxynucleotidyl transferase-mediated deoxyuridine triphosphate nick end labeling (TUNEL) method.**
Results: **The lesions increased in size progressively over the 24 h that followed ablation and the area of the lesion coincided with the area that had been heated above 43°C. TUNEL-positive hepatocytes were surrounded, at some distance, by HSP70-positive hepatocytes were surrounded, at some distance, by HSP70-positive hepatocytes at 6 h, and such cells were in contact with each other at 24 h.**
Conclusions: **Injury to hepatocytes induced by laser ablation increases for 24 h and dying cells express nuclear HSP70, with subsequent fragmentation of DNA. Lasers Surg. Med. 24:14–23, 1999.** **© 1999 Wiley-Liss, Inc.**

Key words: animal model; heat shock protein; laser surgery; Nd:YAG; TUNEL method

INTRODUCTION

Laser-induced thermotherapy (LITT) has been used to treat unresectable localized tumors in the liver, breast, and pancreas [1–3]. In the liver, LITT is applied mostly in cases of liver metastases and, to a limited extent, in cases of unresectable primary hepatocellular carcinoma. It is expected that LITT will be used more widely in the future because it has the advantage of avoiding acute pain, intoxication, possible risk of portal venous thrombosis, and intrahepatic dissemination, as compared with percutaneous ethanol-injection therapy for treatment of hepatic tumors [4].

In the clinical use of LITT, damage to the normal liver adjacent to the tumor should be minimized. The effects of LITT on the liver during and after treatment have been studied sonographically and histopathologically in experimental models in the pig, dog, rabbit, and rat [5–8]. However, the nature of the pathological events that result in coagulation necrosis during the early stages after thermotherapy, in particular, within the first 24 h, remains unknown. It is of fundamental importance for the effective clinical use of LITT that we clarify the mechanisms and processes that induce coagulation necrosis in nor-

*Correspondence to: Hiromu Mori, M.D., Oita Medical University, Hasama-machi, Oita 879-5593, Japan. E-mail: morihrmu@oita-med.ac.jp

Accepted 17 August 1998

mal portions of the liver so that we can predict the final size of laser-induced lesions.

To evaluate damage to tissue by LITT, it is necessary to observe morphological changes at the cellular level using biological markers that reflect the damage to cells and necrosis. Heat-shock protein 70 (HSP70) is a member of the family of stress proteins that are synthesized rapidly in response to stress and, in particular, to sublethal heat shock [9–11]. Since HSP70 is not expressed under normal conditions but is strongly and rapidly expressed after stress, localization of HSP70 might help us to identify cells affected by LITT.

The internucleosomal cleavage of double strands of DNA (DNA fragmentation) is a phenomenon that is typically associated with the initiation of apoptosis. Gavrieli *et al.* [12] proposed that terminal deoxynucleotidyl transferase-mediated (TdT-mediated) deoxyuridine triphosphate (dUTP) nick end labeling (TUNEL) could be used to visualize nuclei with fragmented DNA at the single-cell level in conventional, paraffin-embedded sections of tissue. During thermal damage to tissue, it is unclear whether necrosis and/or apoptosis might play the dominant role. Positive TUNEL signals reflect not only the internucleosomal fragmentation of DNA during apoptosis but also single-strand breaks in DNA during necrosis [13]. Thus by detecting DNA fragmentation in damaged cells, TUNEL provides a useful indicator of dying or dead cells, regardless of the mode of cell death.

In the present study, we examined the chronological development of macroscopic and microscopic alterations in the normal rabbit liver at early stages after laser ablation in an attempt to clarify the mechanisms that promote or interfere with the effects of laser ablation. Furthermore, we investigated the dynamics of possible interactions between direct damage to cells by the laser treatment and the simultaneous response of hepatocytes by immunostaining for HSP70 and application of the TUNEL method.

MATERIALS AND METHODS

Animals and Laser Ablation

Twenty-eight male rabbits, weighing 2.8–3 kg, were treated and sacrificed according to the Guide for the Care and Use of Laboratory Animals of Oita Medical University. The animals were divided into seven groups of four each. All surgical operations and radiological treatments were performed under general anesthesia, which was achieved by intravenous injection of 40 mg/kg sodium pentobarbital (Nembutal; Abbott Laboratories, North Chicago, IL). After opening the abdomen through a midline incision and exposing the liver, we inserted a bare quartz optical fiber (core diameter, 600 μm), with a polished plane-cut tip and 5 mm of jacket and cladding removed, directly into the liver to a depth of 2 cm under ultrasound guidance (SSA, 240A and TUF 73817 7.0 MHz transducer; Toshiba, Tokyo, Japan). A continuous-wave, neodymium-yttrium-aluminum-garnet (Nd:YAG) laser, operating at 1,064 nm (KTP/YAG™ Surgical Laser Systems; Laserscope, San Jose, CA) was used at a power setting of 2 W for 600 sec (1,200 J). The livers of all rabbits were ablated with the laser, via the optical fiber, for 10 min with monitoring of all illumination by real-time ultrasound. Three probes (hypodermic needle microprobes, type MT-23/3) of a thermometer (BAT-10LOP with 3 channels; Physitemp, Clifton, NJ) were fixed in a holder, parallel to each other and at a distance of 3 mm from each other, and the optical fiber for laser ablation was also fixed in the same holder, parallel to the probes, at a shortest distance of 3, 4, or 5 mm. The final distances of the probes from the optical fiber were 3, 6, and 9 mm; 4, 7, and 10 mm; or 5, 8, and 11 mm. The temperature of the tissue was recorded at 1-min intervals during laser ablation, with a 3-min follow-up.

After the laser ablation, the three probes of the thermometer were removed, and a marker tip was inserted parallel to the optical fiber. Both the tip and the optical fiber were cut at a distance of 3 mm from the outside of the liver, affixed to the liver with strong adhesive, and left in the liver. Animals in the first group were sacrificed immediately, and those in the other groups were sacrificed 6 h, 12 h, 24 h, 48 h, and 72 h and 7 days, respectively, after the treatment. The maximum surface area of the thermal lesion was exposed by cutting the liver along the plane determined by the marker tip and the optical fiber. We defined a thermal lesion as a macroscopically discolored lesion (with charring and grayish white discoloration) induced by laser ablation. After photographs had been taken, three needles of 0.8 mm in diameter, set together at a distance of 3 mm from each other, were inserted into the surface of the region perpendicular to the plane as landmarks to indicate the distance from the fiber tip.

Macroscopic and Microscopic Observations

Macroscopic images of the cut surfaces of livers were obtained with a high-resolution digital camera (Nikon, Tokyo, Japan) and transferred to a Macintosh personal computer equipped with PowerPC 601 tip (Apple Computer, Cupertino, CA). The extent of each thermal lesion was measured on respective digital images.

For histopathological examination, resected pieces of liver with landmarks were placed on hard paper-board to prevent bending of the tissue, fixed in 10% formalin, and embedded in paraffin.

The paraffin-embedded sections were cut in a thickness of 4 μm, dewaxed, dehydrated, and stained with hematoxylin and eosin (H&E). In addition to routine histological examination, numbers of nuclei in ten rectangular areas within the thermal lesion were counted on micrographs obtained with a light microscope (BH-2; Olympus, Tokyo, Japan) at high-power magnification. The total number of nuclei in a lesion was estimated as

$$\frac{(\text{number of nuclei per 10 rectangular areas}) \times (\text{the macroscopic size of the thermal lesion})}{(\text{true size of 10 rectangular areas})}.$$

Statistical comparisons among groups were made by one-way analysis of variance (ANOVA) with a posthoc test.

Immunohistochemistry

Dewaxed sections were incubated in 3% hydrogen peroxide for 15 min and then washed in 0.15 M phosphate-buffered saline, pH 7.4 (PBS). For retrieval of antigen, sections were autoclaved in citrate buffer, pH 6.0, at 121°C for 10 min, and allowed to cool to room temperature. After incubation in normal rabbit serum that had been diluted 1:10 with PBS for 10 min, HSP70-specific monoclonal antibody (Stress Gen Biotechnologies, Victoria, BC, Canada), diluted 1:200 with PBS, was applied to the sections, which were then incubated at 4°C for 20 h. The products of the immunoreaction were visualized by the streptavidin-biotin method (SAB kit; Nichirei Corp., Tokyo, Japan) with 3, 3′-diaminobenzidine tetrahydrochloride (DAB) and hydrogen peroxide. Nuclei were counterstained with hematoxylin.

TUNEL Method

Thin sections of paraffin-embedded tissue were dewaxed, dehydrated, and washed in running water. DNA fragmentation was detected with ApopTag (Oncor, Gaithersburg, MD) according to the manufacturer's instruction. The sites of internucleosomal cleavage were labeled by TdT with digoxigenin-coupled dUTP, which was detected by peroxidase-labeled Fab' of sheep IgG raised against digoxigenin. Signals were visualized by incubation with DAB and nuclei were counterstained with hematoxylin.

In order to demonstrate the relationship between the expression of HSP70 and the signals due to TUNEL, we performed double staining, namely, immunostaining for HSP70, as described above, and subsequent TUNEL employing alkaline phosphatase-labeled Fab' of sheep IgG against digoxigenin (Boehringer Mannheim GmbH, Mannheim, Germany) and Vector Blue (Vector Laboratories, Burlingame, CA) or chromogen, without counterstaining of nuclei. The signals specific for HSP70 were dark brown (DAB) and those of TUNEL were blue (Vector Blue).

RESULTS

Temperature During and After Laser Ablation

The temperature was measured at 1-min intervals, in 1-mm increments from 3–11 mm lateral to the tip of the laser fiber. The temperature began to rise just after the start of treatment and remained elevated after 4 min (Fig. 1). The highest temperature of 55°C was measured at the 3-mm point. The maximum temperature during the ablation was >43°C within 7 mm and <40°C beyond 8 mm. After the 10-min treatment, the temperature decreased rapidly and returned to normal within 3 min.

Ultrasound Findings

During and immediately after laser ablation, an elliptical hyperechoic area with a surrounding thin hypoechoic rim was observed around the tip of the laser fiber (Fig. 2a). At 6 h, 12 h, 24 h, 48 h, 72 h, and 7 days, central hyperechoic areas gradually became smaller, whereas outer hypoechoic zones became wider (Fig. 2b).

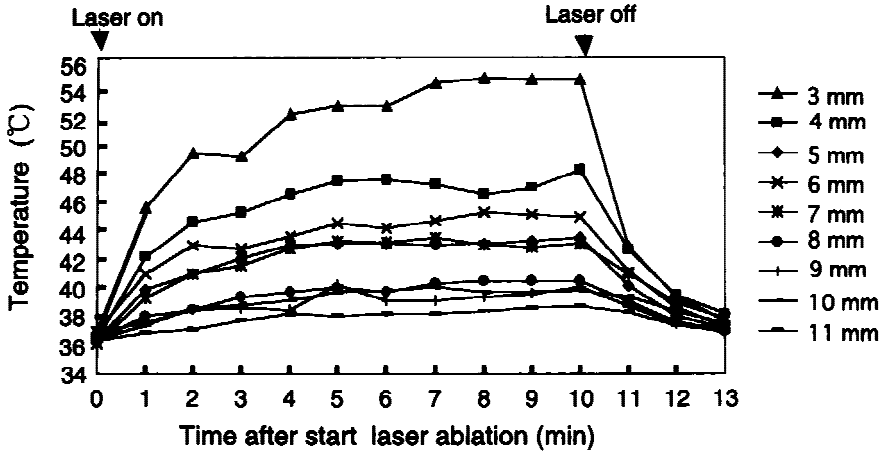

Fig. 1. Temporal and spatial distribution of temperatures after laser ablation. The temperature increased rapidly just after laser ablation and reached a maximum of 55°C at the 3-mm point. It was >43°C within a 7-mm radius and <40°C at the 8-mm point and beyond. The temperature returned to the basal level within 3 min after the end of the ablation.

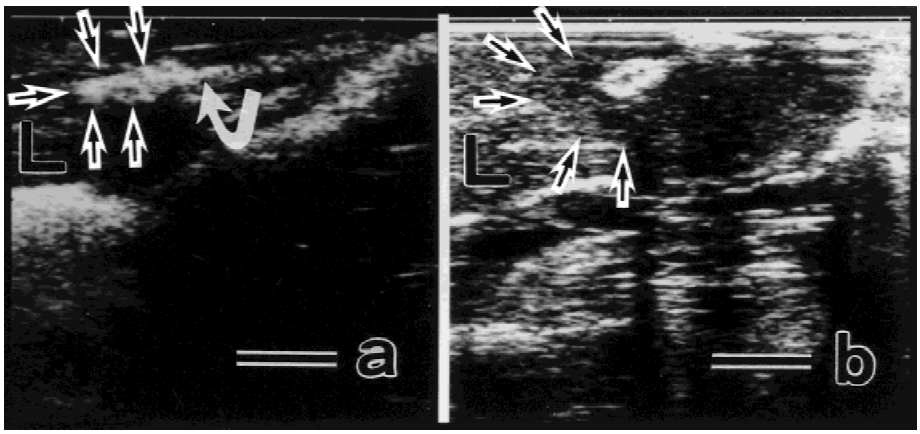

Fig. 2. Ultrasound findings. **(a)** During and immediately after laser ablation, an elliptical hyperechoic area (straight arrows) with a surrounding thin hypoechoic rim was observed around the tip of the laser (curved arrow). **(b)** At 24 h after laser ablation, the central hyperechoic areas became smaller, whereas the outer hypoechoic zone became wider (arrows). L, Liver. Scale bars = 10 mm.

Macroscopic Changes After Laser Ablation

At the macroscopic level, the sections of livers of animals sacrificed immediately after laser ablation showed charring around the fiber tip and grayish white discoloration in the surrounding area (Fig. 3a). On the cut surface, the thermal lesion was elliptical, extending from the center of the fiber tip in the direction of ablation. Hemorrhage or congestion was observed in the zone around the lesion just after treatment and remained evident for 24 h. These findings were more distinct 12 h after treatment (Fig. 3c), and the demarcation between the intact and damaged liver tissue was clear at 24 h (Fig. 3d).

The thermal lesion gradually increased in size to reach a maximum 24 h after laser ablation. The volume was then approximately three times that of the initial lesion immediately after the treatment (Fig. 4). The area of the lesion was unchanged after 48 h and appeared to be slightly smaller at 7 days, although the difference was not statistically significant. The lesions in animals in the 7-day group were clearly encapsulated by granulation tissue. The maximum size of thermal lesions 24 h after laser ablation coincided with the

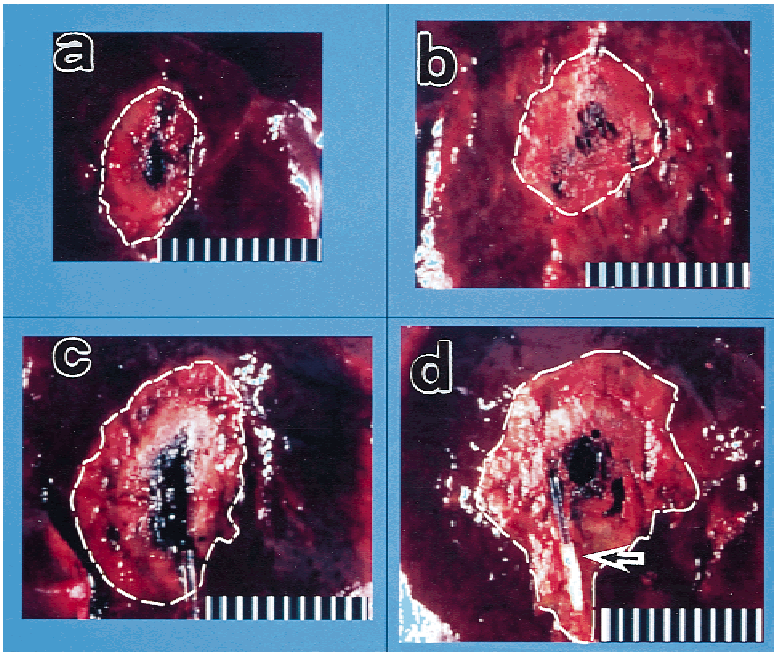

Fig. 3. Macroscopic changes in the lesion induced by laser ablation. Charring and vacuolization are seen at the center of the thermal lesion (white line), which was larger at 6 h than the initial lesion just after ablation. **(a–d),** just after, 6 h, 12 h, and 24 h after laser ablation, respectively. Arrow indicates a quartz fiber. Scale bars = 10 mm.

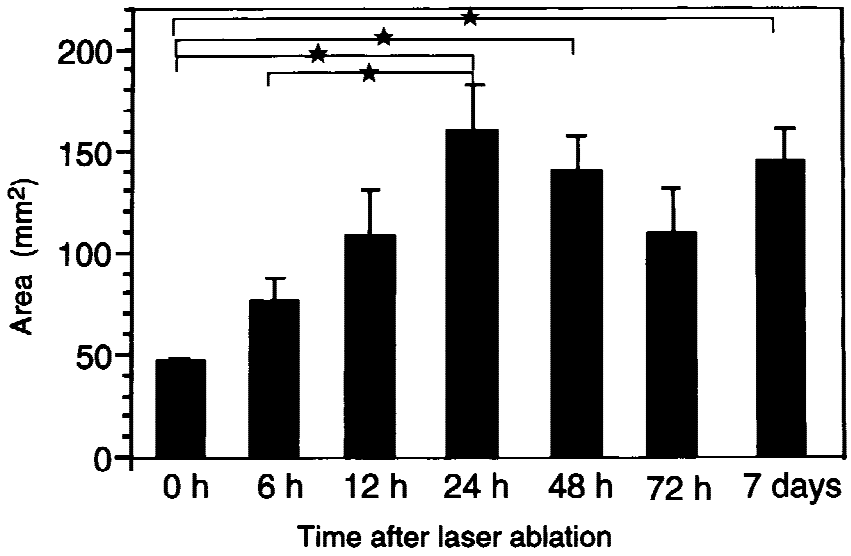

Fig. 4. Changes in the area of the thermal lesion. The area of the thermal lesion increased significantly with time and reached a maximum 24 h after laser ablation. Then it decreased gradually. Values are means ± SE of results from four animals in each group. *, $P < 0.05$.

area within a 7-mm radius of the fiber tip at the completion of laser ablation (>43°C).

Histological Observations

Just after laser ablation, congestion was seen at the periphery of the discolored region observed on macroscopic images, and numerous erythrocytes were packed in the sinusoids (Fig. 5a). The cytoplasm of hepatocytes in the central area of the damaged liver tissue was slightly eosinophilic and the nuclei of the hepatocytes appeared to be reduced in size. The extent of con-

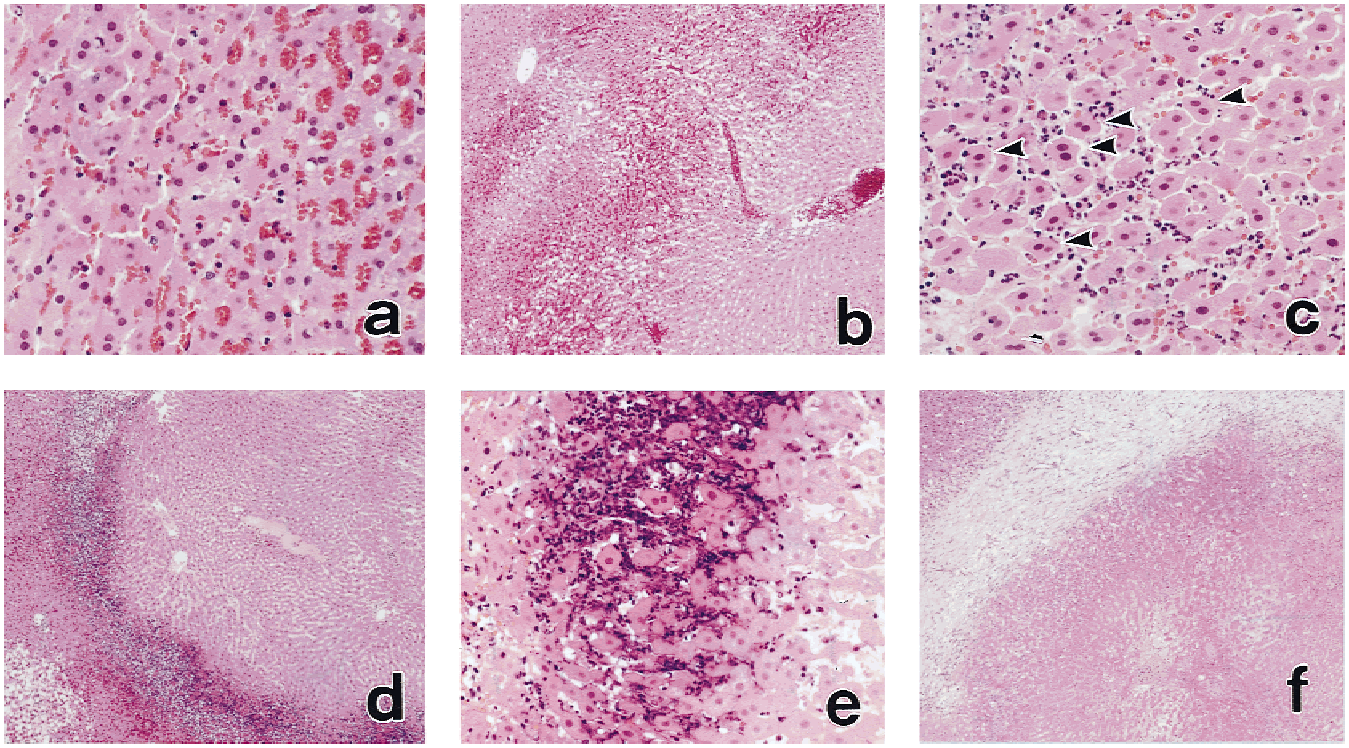

Fig. 5. Microscopic changes after laser ablation. **(a)** Sinusoidal congestion was initially observed at the periphery of the thermal lesion just after laser ablation. H&E, ×180. **(b)** Congestion increased in degree and extent after 6 h. H&E, ×40. **(c)** Binucleated hepatocytes (arrowheads) were seen in the marginal zone at 12 h, with infiltration by a few neutrophils. H&E, ×180. **(d)** These features were prominent, with a zonal distribution, at 24 h. H&E, ×40. **(e)** Both peripheral and central hepatocytes in the lesion gradually became ghost cells from 12–48 h. H&E, ×180. **(f)** Finally, the lesion was occupied by necrotic hepatocytes and surrounded by dense connective tissue at 7 days. H&E, ×40.

gestion increased progressively, with marked dilatation of the sinusoids in the marginal zone between the intact and damaged liver tissue 6 h after the treatment. (Fig. 5b). A small number of neutrophils was observed in the marginal zone at 12 h, and binucleated hepatocytes of irregular shape were occasionally seen in this zone (Fig. 5c). The lesion was clearly delineated by zonal infiltration of neutrophils, and the central portion of the damaged tissue was more eosinophilic than the surrounding intact liver tissue at 24 h (Fig. 5d). The damaged hepatocytes progressively lost their nuclei and began to resemble ghost cells from 12–72 h (Fig. 5e). Most hepatocytes in the lesion appeared to be involved in coagulation necrosis 7 days after treatment, and the marginal zone was clearly encapsulated by fibrous granulation tissue that consisted of connective tissue, fibroblasts, capillaries, and a few inflammatory cells (Fig. 5f).

As the thermal lesion increased in size, we counted the number of hepatocytes within the lesion to determine whether the expansion of the lesion was caused by swelling of damaged hepatocytes and dilatation of the sinusoid, or whether it reflected a true increase in numbers of damaged hepatocytes that occupied the lesion. The estimated number of hepatocyte nuclei per unit area increased continuously from just after the laser ablation to reach a maximum at 24 h. The maximum number was more than three times the original number. Thereafter, the number decreased gradually because of hepatocytic necrosis (Fig. 6), which was complete within 7 days after treatment.

Immunostaining for HSP70 and TUNEL

Intranuclear HSP70 was detected in hepatocytes and in biliary epithelial cells located adjacent to the thermal lesion 6 h after laser ablation (Fig. 7a). The immunostaining for HSP70 increased in intensity and the number of immuno positive hepatocytes increased from 12–24 h after treatment (Fig. 7c,d). HSP70-positive hepatocytes were recognized in a concentrically expanding region of the originally damaged liver tissue and

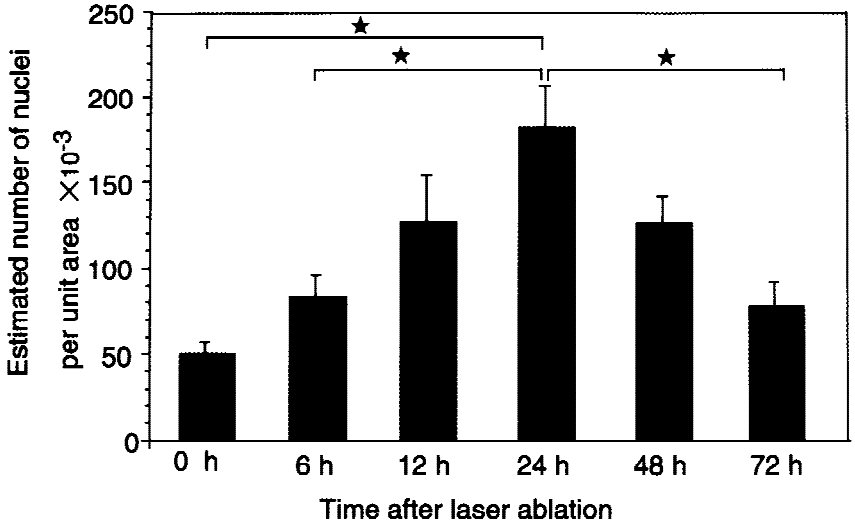

Fig. 6. Numbers of nuclei in the thermal lesion. The number of hepatocyte nuclei increased from just after laser ablation for 24 h and decreased gradually thereafter. Nuclei could not be counted at 7 days because of complete necrosis of the damaged liver tissue. Values are means ± SE of results from four animals in each group. *, $P < 0.05$.

made contact with the external margin of the lesion at 24 h (Fig. 7d). Immunoreactive HSP70 was scarcely observed in the nuclei of hepatocytes at 48 h (Fig. 7e), and it had disappeared at 72 h (Fig. 7f).

Cells with positive TUNEL were seen among the perivascular hepatocytes and in the biliary epithelium located relatively far from the lesion and among hepatocytes located inside the marginal zone 6 h after laser ablation (Fig. 7b). The marginal hepatocytes with positive TUNEL reaction expanded concentrically at 12 h and 24 h (Fig. 7c,d), but TUNEL-positive cell disappeared within 7 days after the treatment. With expansion of the lesion, perivascular hepatocytes, and biliary epithelial cells, located relatively far from the lesion, that gave a positive TUNEL reaction at 6 h were included in the elliptically expanded lesion. Both TUNEL-positive and HSP70-positive cells were located around the marginal zone 6–24 h after laser ablation. The former cells were surrounded by the latter ones with some distance between them at 6 h (Fig. 7a,b). Double staining indicated that they were contiguous at 12 h (Fig. 7c) and made contact with each other at 24 h (Fig. 7d).

DISCUSSION

In the clinical setting, LITT is performed with ultrasonographic identification of the target lesion. The area treated LITT is detected as an elliptical hyper- or hypoechoic image [14–16]. To compare the macroscopic damage to tissue with the ultrasonographic image, it is appropriate to evaluate tissue damage in terms of area rather than maximum diameter. In the present study, therefore, we used computer-assisted measurements of the areas of thermal lesions, a method that would be useful for analysis of ultrasonographic images.

An apparent macroscopic change, such as discoloration, should be verified by histological examination. However, fixation formalin and embedding in paraffin result in shrinkage, which causes problems in attempts to compare macroscopic and microscopic measurements. For macroscopic observations, we made tiny holes in tissues to serve as landmarks. In addition, we employed thermal sensors to obtain concurrent temperatures at precise distances from the laser. Such devices can be expected to be very useful for evaluation of injured areas after laser ablation.

Chronological changes in thermal lesions within the first 24 h after laser ablation have not been reported in the literature, to our knowledge, and most reported measurements of lesions were made on the day of or more than 1 day after treatment [17,18]. In the present study, the thermal lesion increased in area to three times the initial area of the lesion within 24 h after treatment. Estimated numbers of nuclei in the lesion also increased. It seems likely that the expansion of lesions was caused by progressive degeneration of cells and not by swelling of degenerated cells or interstitial edema.

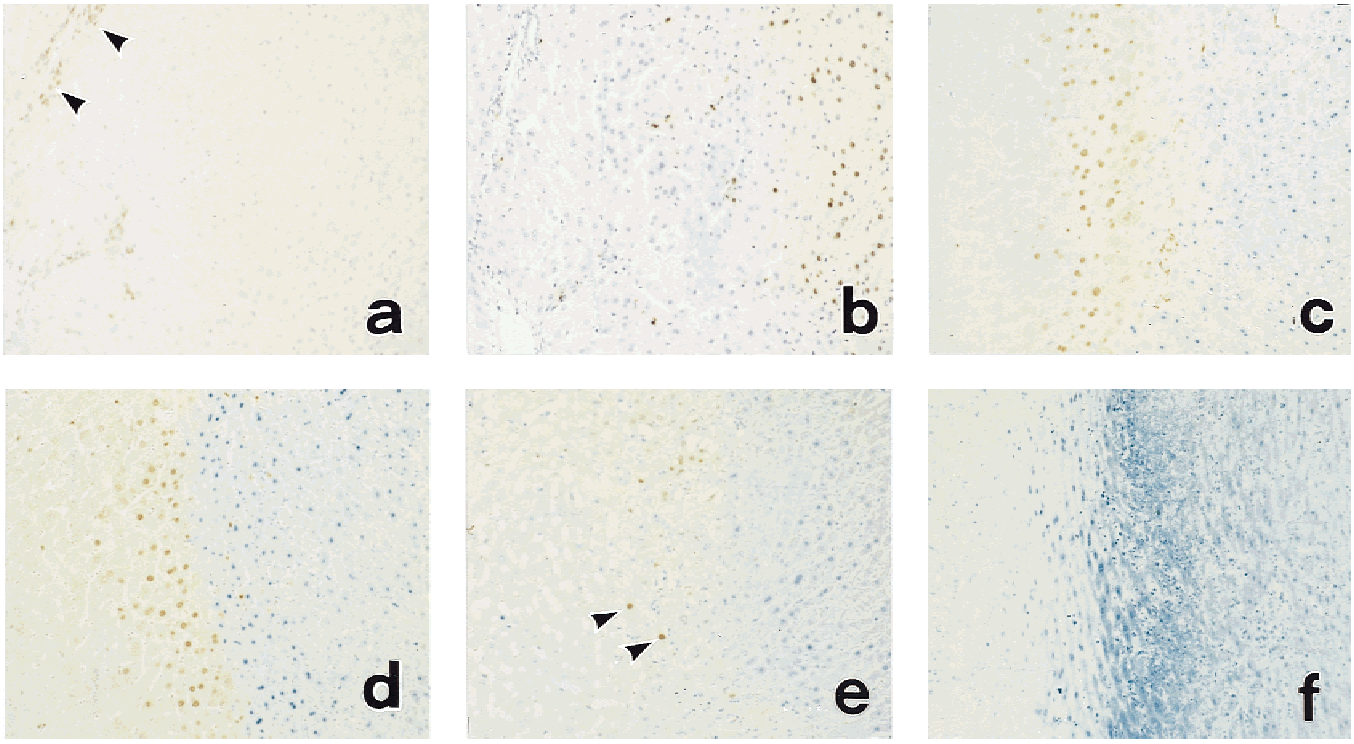

Fig. 7. Results of immunostaining for HSP70 and the TUNEL method. TUNEL-positive cells were located separately from the area of HSP70-positive cells, which included cells of the biliary epithelium (arrowheads) and a few hepatocytes 6 h after laser ablation, as shown in **(a)** and **(b).** Double staining revealed positive cells contiguous to and in contact with each other from 12–24 h after the treatment, as shown in **(c)** and **(d).** The HSP70-positive cells were seen just beyond TUNEL-positive cells at 48 h (**e,** arrowheads) and had completely disappeared at 72 h **(f),** but TUNEL-positive cells remained visible in the marginal zone from 48–72 h, as shown in (e) and (f). (a) Immunostaining for HSP70; (b) TUNEL method; (c–f), double staining, i.e., immunostaining for HSP70 and TUNEL. ×90.

Mailhos et al. [19] suggested that the induction of HSP70 might be responsible for the protective effect of heat shock on apoptosis in neuronal cells. Laszlo et al. [20,21] reported that heated fibroblasts in culture express HSP70, which reaches a maximum level at 8 h, and they proposed that HSP70 might play a direct role in repairing heat-damaged cells. In the present study, the HSP70-positive cells in the marginal zone, 24 h after treatment, were considered to have acquired thermal resistance that allowed them to escape from cell death since the region of cell death did not expand after 24 h. In contrast, the HSP70-positive cells found within 24 h, which had been heated above 43°C, were unable to escape cell death. This phenomenon might have been due to the fact that heat shock at temperatures >43°C induced HSP70 in this region, but was too strong to induce thermotolerance.

The TUNEL method allows detection of the fragmentation of DNA. However, when the TUNEL method is used to evaluate damage to cells, it is difficult to determine whether positively stained cells are apoptotic or necrotic [13,22]. In the present study, we considered that all TUNEL-positive cells would eventually die.

Analysis of survival of mammalian cells after heating, by construction of Arrhenius plots, revealed an inflection point near 43°C, and increased numbers of cells were killed by heating above 43°C [23]. In the present study, the cells in the area heated above 46°C for 8 min (within a radius of 4 mm) died just after the treatment. The maximum damage coincided with the area that had been heated above 43°C (within a radius of ~7 mm). In this area, most of the hepatocytes ultimately became TUNEL-positive and gradually died within 24 h. Necrosis was finally evident in the thermal lesion that included these cells at 7 days. The TUNEL-positive cells were surrounded by HSP70-positive cells after 6 to 24 h. HSP70 appeared in the epithelium of the biliary tract and in a few hepatocytes at 6 h, when TUNEL-positive cells were located separately from the area of HSP70-positive cells. Thereafter, with expansion of the lesion, TUNEL-positive hepatocytes were

seen closer to the HSP70-positive cells and they made contact with them 24 h after treatment. We suggest that synthesis of HSP70 might occur sooner than cleavage of DNA because damaged cells were positive for HSP70 first and only later were they TUNEL-positive. Expression of HSP70 might be proof of that a cell has been heated >43°C, and it is known that some fatal reactions of cells, such as apoptosis, are activated at 43–50°C. Thus the fragmentation of DNA that was detected by the TUNEL method might occur as a late event and as a result of a fatal reaction to heat shock.

The fate of HSP70-positive cells might be modified by other factors: abnormal blood flow, reperfusion, free radicals, nitric oxide, and so on. Nuutinen et al. [24] suggested that the progression of tissue destruction within 24 h after laser exposure might be due to vascular shutdown by thrombosis of vessels, as well as to thermal damage, in an experimental model of pancreatic cancer in hamsters. In our experimental model, neutrophils infiltrated the marginal zone, which increased in size concentrically. Thus factors associated with infiltrating neutrophils might have influenced cell death, in addition to the initial thermal stimulus.

The present study demonstrated that the extent of injury to hepatocytes induced by laser ablation increases for 24 h and that dying cells express nuclear HSP70, with the subsequent fragmentation of DNA. Immunostaining for HSP70 and the TUNEL method appear to be useful methods for clarifying the effects of LITT in the liver. For further clinical use of LITT, it is now necessary to investigate whether similar histopathological changes occur in hepatocellular carcinoma and in metastatic liver tumors after laser ablation.

REFERENCES

1. Bown SG. Phototherapy of tumors. World J Surg 1983; 7:700–709.
2. Masters A, Steger AC, Bown SG. Role of interstitial therapy in the treatment of liver cancer. Br J Surg 1991; 78:518–523.
3. Amin Z, Donald JJ, Masters A, Kant R, Steger AC, Bown SG, Lees WR. Hepatic metastases: Interstitial laser photocoagulation with real-time US monitoring and dynamic CT evaluation of treatment. Radiology 1993; 187:339–347.
4. Amin Z, Bown SG, Lees WR. Local treatment of colorectal liver metastases: a comparison of interstitial laser photocoagulation (ILP) and percutaneous alcohol injection (PAI). Clin Radiol 1993; 48:166–171.
5. Dachman AH, McGehee JA, Beam TE, Burris JA, Powell DA. US-guided percutaneous laser ablation of liver tissue in a chronic pig model. Radiology 1990; 176:129–133.
6. Malone DE, Wyman DR, Moote DJ, DeNardi FG, Mori H, Swift C, Lewis R, Stevenson GW, Wilson BC. Sonographic changes during hepatic interstitial laser photocoagulation: An investigation of three optical fiber tips. Invest Radiol 1992; 27:804–813.
7. Steger AC, Lees WR, Shorvon P, Walmsley K, Bown SG. Multiple-fiber low-power interstitial laser hyperthermia: Studies in the normal liver. Br J Surg 1992; 79:139–145.
8. Van Hillegersberg R, de Witte MT, Kort WJ, Terpstra OT. Water-jet-cooled Nd:YAG laser coagulation of experimental liver metastasis: Correlation between ultrasonography and histology. Lasers Surg Med 1993; 13:332–343.
9. Beck SC, Paidas CN, Tan H, Yang J, De Maio A. Depressed expression of the inducible form of HSP70 (HSP72) in brain and heart after in vivo heat shock. Am J Physiol 1995; 269:608–613.
10. Vidair CA, Huang RN, Doxsey SJ. Heat shock causes protein aggregation and reduced protein solubility at the centrosome and other cytoplasmic locations. Int J Hyperthermia 1996; 12:681–695.
11. Manzerra P, Rush SJ, Brown IR. Tissue-specific differences in heat shock protein hsc70 and hsp70 in the control and hyperthermic rabbit. J Cell Physiol 1997; 170:130–137.
12. Gavrieli Y, Sherman Y, Ben-Sasson SA. Identification of programmed cell death in situ via specific labeling of nuclear DNA fragmentation. J Cell Biol 1992; 119:493–501.
13. Grasl-Kraupp B, Ruttkay-Nedecky B, Koudelka H, Bukowska K, Bursch W, Schulite-Hermann R. *In situ* detection of fragmented DNA (TUNEL assay) fails to discriminate among apoptosis, necrosis, and autolytic cell death: A cautionary note. Hepatology 1995; 21:1465–1468.
14. Steger AC, Shorvon P, Walmsley K, Chisholm R, Bown SG, Lees WR. Ultrasound features of low-power interstitial laser hyperthermia. Clin Radiol 1992; 46:88–93.
15. Nolsøe CP, Torp-Pedersen S, Burcharth F, Horn T, Pedersen S, Christensen N-E. H, Olldag ES, Andersen PH, Karstrup S, Lorentzen T, Holm HH. Interstitial hyperthermia of colorectal liver metastases with a US-guided Nd-YAG laser with a diffuser tip: A pilot clinical study. Radiology 1993; 187:333–337.
16. Van Hillegersberg R, Van Staveren HJ, Kort WJ, Zondervan PE, Terpstra OT. Interstitial Nd:YAG laser coagulation with a cylindrical diffusing fiber tip in experimental liver metastases. Lasers Surg Med 1994; 14:124–138.
17. Malone DE, Wyman DR, DeNardi FG, McGrath FP, De Gara CJ, Wilson BC. Hepatic interstitial laser photocoagulation: An investigation of the relationship between acute thermal lesions and their sonographic images. Invest Radiol 1994; 29:915–921.
18. Löfberg A-M, Arvidsson D, Andersson T, Lindgren PG, Lörelius L-E, Nordlinder H. Ultrasound-monitored laser-induced local hyperthermia in the liver. An experimental study on pigs. Acta Radiol 1994; 35:6–9.
19. Mailhos C, Howard MK, Latchman DS. Heat shock protects neuronal cells from programmed cell death by apoptosis. Neuroscience 1993; 55:621–627.
20. Laszlo A. The relationship of heat-shock proteins, ther-

motolerance, and protein synthesis. Exp Cell Res 1988; 178:401–414.
21. Ohtuka K, Laszlo A. The relationship between hsp 70 localization and heat resistance. Exp Cell Res 1992; 202:507–518.
22. Charriaut-Marlamgue C, Ben-Ari Y. A cautionary note on the use of the TUNEL stain to determine apoptosis. NeuroReport 1995; 7:61–64.
23. Bauer KD, Henle KJ. Arrhenius analysis of heat survival curves from normal and thermotolerant CHO cells. Radiat Res 1979; 78:251–263.
24. Nuutinen P, Eskelinen M, Surakka M, Marin S, Alhava E. Low power interstitial hyperthermia in the treatment of ductal carcinoma of the pancreas: An experimental study with Syrian gold hamsters. Lasers Med Sci 1992; 7:45–48.